

# Features of electron-beam sintering of Al<sub>2</sub>O<sub>3</sub>-Ti composite ceramics in the forevacuum pressure range

A S Klimov, I Yu Bakeev, E M Oks, V T Tran and A A Zenin

Physics Department, Tomsk State University of Control Systems and Radioelectronics, 634050, Tomsk, Russia

E-mail: klimov680@gmail.com

**Abstract.** The article presents electron-beam sintering of composite cermets based on aluminum oxide and titanium. An electron beam generated by a forevacuum plasma electron source for sintering was used. The sintering samples were made from fine-grained powders and compressed by uniaxial pressing. It is shown that when heated to 1600 °C, a powder mixture with a ratio of aluminum oxide of 50% (wt.) and 50% titanium (wt.) large pores are formed in the sample. Measurements of the emission spectrum of the beam plasma formed above the surface of the irradiated sample showed the presence of aluminum. This may be due to the evaporation of these components during electron beam irradiation.

## 1. Introduction

Aluminum oxide ceramics are characterized by excellent wear resistance and hardness, as well as high thermal and chemical stability [1, 2]. The combination of unique properties of this material attracts great interest in industrial applications of aluminum oxide ceramics, such as biomaterials, aerospace, nuclear power, automobiles and electronics [3-5]. However, the use of composite as a structural material has been limited due to its low fracture toughness and low crack resistance. To overcome the fragility of monolithic ceramics, metal-ceramic composites were developed. It has been proved that the inclusion of metal reinforcing materials in the Al<sub>2</sub>O<sub>3</sub> matrix is an effective way to increase the impact strength of ceramics[6]. The most obvious advantage of cermet is that it can advantageously combine in one material the heterogeneous properties of ceramic and metal components. When metal particles are incorporated into the ceramic matrix, the composite is armored by external reinforcement mechanisms, such as crack overlap or crack deflection, which can lead to increased fracture resistance [7].

Despite the success in obtaining metal-ceramic composites, there are still difficulties associated with obtaining such compounds with sufficient mechanical strength. This is due to a large difference in the physical and mechanical properties of ceramics and metals, such as the coefficient of thermal expansion, chemical composition and modulus of elasticity [8]. In addition, not all metals are suitable for inclusion in the matrix of aluminum oxide ceramics due to poor wettability of ceramics. The most suitable materials are active metals such as Ti, Zr, Ni or V [9, 10], which significantly increase the wettability and spreadability of the liquid metal in ceramics. Ti is a typical active element that contributes to the wetting and adhesion of aluminum oxide ceramics [11].

There are various ways to create metal-ceramic materials – such as reactive metal infiltration [12, 13], reactive metal penetration [14], hot pressing [15], high-energy ball milling [16]. Recently developed spark plasma sintering (SPS) [17, 18] due to the increased heating rates allows you to achieve a high relative density in a very short time. However, this method can only sinter samples of a certain shape



and size. Each of these methods has its advantages and disadvantages and may not be applied to all types of composite materials. In addition, most of these processes are expensive, have low productivity, and are complex in their procedures and controls.

Despite the wide variety of methods for producing cermets, new methods are still being sought. One such method may be electron-beam sintering in the forevacuum pressure range. A narrowly focused electron beam propagating in vacuum at pressures from units to tens of Pascals [19] is able to quickly heat the surface of the workpiece to a temperature of more than 2000°C. The plasma formed during the propagation of the beam in the gas neutralizes the negative charge of the surface irradiated by the electron beam [20]. Plasma electron sources are successfully used for sintering ceramics, electron-beam welding of metal-ceramic units, processing of quartz glass, creating functional gradient materials and other technologies for processing dielectrics [21-23]. Previously, we have shown in [24] the principal possibility of creating metal-ceramic FGM materials based on aluminum oxide and titanium.

This article is aimed at studying the influence of titanium content on the production of uniformly sintered metal-ceramic material. In this work, we use electron-beam irradiation in the forevacuum pressure range for sintering cermets.

## 2. Materials and methods

The experiments were carried out using a plasma electron source, a schematic image of which is shown in Figure 1. The design and parameters of the electron source and electron beam are presented in [25]. In this work, the following parameters of the electron beam were used: the beam current varied from 15 to 45 mA, the accelerating voltage from 2 to 10 kV, the beam diameter was 0.5 mm. The plasma electron source was placed on the flange of the vacuum chamber. All the experiments were in the medium of helium. The choice of helium is due to its chemical inertness.

The sintering samples were made from fine-grained aluminum oxide and titanium powders. The average particle size of aluminum oxide powder was 100  $\mu\text{m}$ , the average particle size of titanium powder was 30  $\mu\text{m}$ . Three types of samples were made. Sample 1 contained 100% aluminum oxide, sample 2 contained 50% (wt.) aluminum oxide and 50% (wt.) titanium, sample 3 consisted of 100% titanium. Cold static pressing in a closed mold was used.

Parameters of samples before sintering are presented in table 1. For the sintering process, the sample was placed on a graphite crucible. The crucible design provided a minimal heat sink to increase the efficiency of electron beam energy transfer to the irradiated sample. Graphite was chosen because of its high melting point (more than 3800 °C), as well as its ease of processing.

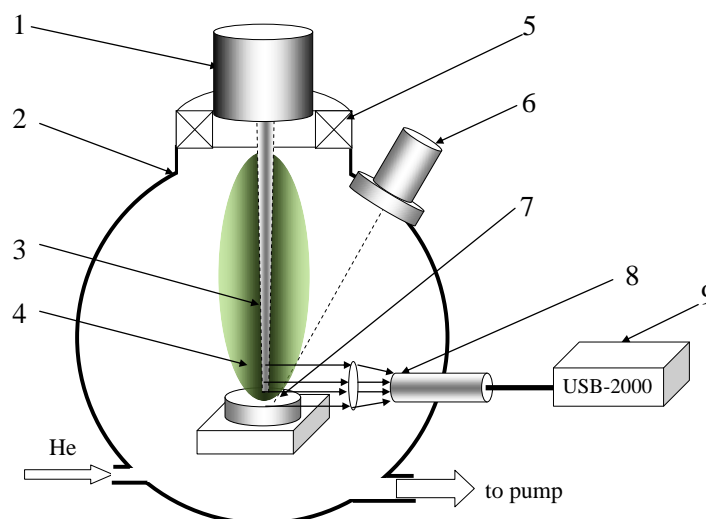


**Figure 1.** Experimental setup: 1 – plasma source of a focused electron beam, 2 – vacuum chamber, 3 – electron beam, 4 – electron beam plasma, 5 – magnetic focusing and deflecting coils, 6 – infrared pyrometer, 7 – sintered sample, 8 – fiber optic cable, 9 – optical spectrometer.

The vacuum chamber was pumped to a pressure of 3 Pa, after which the chamber was filled with helium to a pressure of 30 Pa. The sample was heated by an electron beam for 20-25 minutes. The heating rate was 80 deg/min. When the temperature of the treated surface reached 1600°C the heating stopped and the sample was kept at a constant temperature for 10 minutes. The surface temperature of the sample was controlled by an infrared pyrometer 5 RAYTEK 1 NM (Raytek Corporation, USA). The range of measurement of temperature by pyrometer from 550 °C to 3000 °C. After isothermal exposure, the electron beam power was reduced for 20 minutes. The cooling rate was 100 deg/min. After switching off the plasma electron source, the sample was cooled in vacuum for 10-15 minutes. A spectrometer (Ocean Optics USB-2000, USA) with a resolution of 0.3 nm was used to measure the emission spectrum (200-800 nm) of the beam plasma. The input of radiation into the spectrometer was carried out by a fiber-optic cable, which was located close to the irradiated sample. The microstructure of the samples after sintering were studied by optical microscope.

**Table 1.** The parameters of the samples before sintering.

Sample 1		Sample 2		Sample 3	
Al <sub>2</sub> O <sub>3</sub> , mass.%	Ti, mass.%	Al <sub>2</sub> O <sub>3</sub> , mass.%	Ti, mass.%	Al <sub>2</sub> O <sub>3</sub> , mass.%	Ti, mass.%
100	0	50	50	0	100

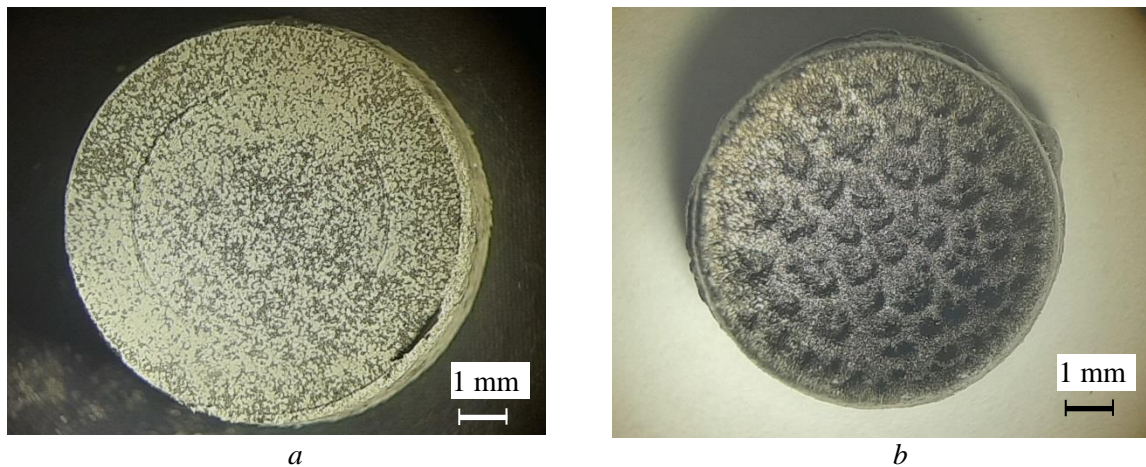
### 3. Experimental results and discussion

Table 2 shows the parameters of the samples after electron-beam sintering for 10 minutes at a constant temperature of 1600 °C. As can be seen from table 1, the volume of all samples after sintering decreased and the density increased. The largest relative change in density after sintering was in the sample 1 consisting of aluminum oxide (density increased by more than 70%). The mass of sample 2 and its thickness decreased more compared to the other samples. Such a significant change in the mass of the sample 2 after sintering looks unexpected because the temperature to which the surface was warmed up is not sufficient for evaporation. As is known, the boiling point of aluminum oxide and titanium is more than 3500 °C, which is much higher than the temperature reached in the experiment.

**Table 2.** Sample parameters before and after sintering.

	Sample 1		Sample 2		Sample 3	
	before	after	before	after	before	after
<i>m</i> , g	0.554	0.505	0.921	0.769	0.906	0.906
<i>d</i> , mm	10.21	8.23	10.17	9.3	10.25	9.14
<i>h</i> , mm	3.55	2.87	5.42	3.5	4.95	4.38
$\rho$ , g/cm <sup>3</sup>	1.906	3.308	2.092	3.235	2.218	3.153

Photos of the surface of the sample 2 before and after sintering are shown in figure 2. As can be seen from the photos, after sintering, deep craters were formed on the surface of sample 2, located fairly evenly.



**Figure 2.** Photo of the surface of sample 2 before (a) and after (b) sintering.

The ordered arrangement of the craters can be explained by the features of scanning the electron beam on the surface of the sample. The fact is that when scanning the electron beam does not move continuously, but discretely, though with a fairly small step of sampling. Thus, at certain time intervals, the electron beam does not move, but irradiates the sample surface locally. At this point of the surface, it is possible to achieve a higher temperature than the general surface temperature and, consequently, the evaporation of the elements included in the sample. Possible confirmation of this statement can be emission spectra of the beam plasma. Such plasma is formed by ionization of a gas of the vacuum chamber with accelerated electrons of the beam. In addition to the residual gas molecules, the molecules of the substance vaporized from the irradiated surface can also be ionized.

Figure 3 shows the emission spectrum of a beam plasma at a sample surface temperature of 500 °C (1) and 1500 °C (2). A solid section of the spectrum in Figure 3 (2) occurs due to a partial hit of radiation from the heated crucible and the sample on the spectrometer. The most intense lines of the spectrum are helium (501.5 nm). There are weak lines of nitrogen, oxygen, and titanium and aluminum. The presence of nitrogen is associated with incomplete removal when pumping the chamber and purging it with helium.

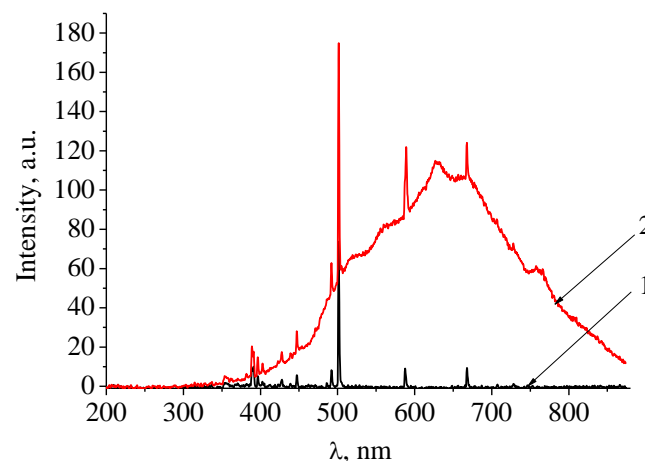


**Figure 3.** Emission spectrum of the beam plasma under electron-beam irradiation of the sample 2: 1 – surface temperature of 500 °C, 2 – surface temperature of 1500 °C.

As it was suggested above, when irradiated with an electron beam, local heating of the surface and evaporation of the elements that make up the sample can occur. Figure 4 shows the dependence of the

line intensity of 396.52 nm (Al), as well as the dependence of the surface temperature of sintered samples 2 and 3 on time.

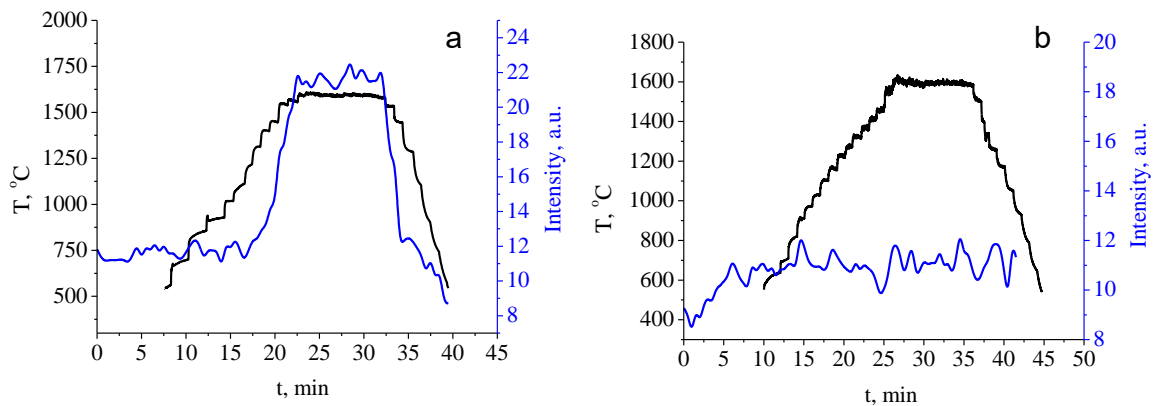


**Figure 4.** Dependence of the surface temperature (black) of sample 2 (a) and sample 3 (b) and the intensity (blue) of the line 396.52 nm on the time of electron-beam irradiation.

As can be seen from figure 4 for sample 2, the intensity changes in the same way as the temperature - as the temperature increases, the intensity increases, and as the sample cools, the intensity decreases. The reason may be that in the sample 2 containing  $\text{Al}_2\text{O}_3$  occurs evaporation of aluminum or its compounds. The radiation of aluminum atoms that are part of the vaporized aluminum oxide is detected by a spectrometer. For sample 3, the intensity of line 396.52 nm does not have such a strong dependence on temperature and time. For sample 3 consisting of titanium, such as would be expected, is not observed and the surface of sample 3 does not contain pores, Figure 5.



**Figure 5.** Photo of the surface of sample 3.

Thus, when sintering a powder mixture of aluminum oxide ceramics and titanium with a ratio of components 1:1, the local temperature value may exceed the melting point Ti or  $\text{Al}_2\text{O}_3$ . Low thermal conductivity of aluminum oxide ceramics leads to its heating to evaporation temperature. Intense evaporation of  $\text{Al}_2\text{O}_3$  leads to the formation of craters in the sintered material. The selection of sintering modes is necessary-it is possible to increase the time of isothermal exposure and simultaneously reduce the sintering temperature. It should be noted that sintering of materials with discretely varying aluminum oxide content over the sample thickness allows obtaining gradient materials under the same irradiation modes [24].

#### 4. Conclusion

As a result of the study, samples of composite ceramics containing aluminum oxide and titanium with a ratio of 1:1 were obtained. It is shown that under electron-beam irradiation at an exposure temperature of 1600 °C, intensive evaporation of aluminum oxide ceramics from the sample surface occurs. The reason for this may be in the inhomogeneous local heating of the surface when it is scanned by an electron beam. This fact must be taken into account when sintering composite materials.

#### Acknowledgments

The work is supported by the Ministry of science and higher education of the Russian Federation – grant of the President for doctors of Sciences No 075-15-2019-372.

#### References

- [1] Shackelford J F and Doremus R H 2010. Ceramic and Glass Materials: Structure, Properties and Processing *New York: Springer*
- [2] Lide D R (editor) 2009 Handbook of Chemistry and Physics. 90th ed. *CRS Press*.
- [3] Xin C, Liu W, Li N, Yan J, Shi S-Q 2016 *Ceram. Int.* **42** 9599.
- [4] Kar A, Mandal S, Venkateswarlu K, Ray A K 2007 *Mater. Charact.* **58** 555.
- [5] Li J, Pan W, Yuan Z, Chen Y 2008 *Appl. Surf. Sci.* **254** 4584.
- [6] Ighodaro O L and Okoli O I 2008 *International Journal of Applied Ceramic Technology* **5**(3) 313.
- [7] Raddatz O, Schneider G A, Mackens W, Voss H, Claussen N 2000 *J. Eur. Ceram. Soc.* **20**:2261.
- [8] Park J-W, Mendez PF, Eagar T W 2005 *Scr. Mater.* **53** 857.
- [9] Bian H, Fu W, Lei Y, Song X, Liu D, Cao J, Feng J 2018 *Ceram. Int.* **44** 11456.
- [10] Kozlova O, Braccini M, Voytovych R, Eustathopoulos N, Martinetti P, Devismes M-F 2010 *Acta Mater.* **58** 1252.
- [11] Kritsalis P, Drevet B, Valignat N, Eustathopoulos N 1994 *Scr. Metall. Mater.* **30** 1127.
- [12] Breslin M C, Ringnalda J, Seeger J, Marasco A L, Daehn G S, Fraser H L 1994 *Ceram. Eng. Sci. Proc.* **15**(4) 104.
- [13] Wu S, Gesing A J, Travitzky N A, Claussen N 1991. *J. Eur. Ceram. Soc.* **7** 277.
- [14] Naga S M, El-Maghraby A, El-Rafei A M 2007. *Am. Ceram. Soc. Bull.* **86** 9301.
- [15] Ellerby D T, Loehman R E 2000 *Ceram. Eng. Sci. Proc.* **21** 659.
- [16] Günther R, Klassen T, Dickau B, Gärtner F, Bartels A, Bormann R 2001 *J. Am. Ceram. Soc.* **84** 1509.
- [17] Fujii T, Tohgo K, Iwao M, Shimamura Y 2018 *Journal of Alloys and Compounds* **744** 759.
- [18] Gutierrez-Gonzalez C F, Fernandez-Garcia E, Fernandez A, Torrecillas R, Lopez-Esteban S 2014 *Journal of Materials Science* **49**(10) 3823.
- [19] Burdovitsin V A, Goreev A K, Klimov A S, Zenin A A, Oks E M 2012 *Technical Physics* **57**(8) 1101
- [20] Bakeev I Y, Dvilis E S, Klimov A S, Oks E M, Zenin A A 2018 *Journal of Physics: Conference Series* **945** 012016.
- [21] Zenin A A, Klimov A S, Oks E M 2018 *Ceramics International* **45**(4) 4798.
- [22] Klimov A S, Bakeev I Y, Dvilis E S, Oks E M, Zenin A A 2019 *Vacuum* **169** 108933.
- [23] Klimov A S, Zenin A A, Bakeev I Y, Oks E M 2019 *Russian Physics Journal* **62**(7) 1123
- [24] Klimov A S, Zenin A A, Tu T V, Bakeev I Y 2019 *Journal of Physics: Conference Series* **1393** 012096.